Re-evaluating the p7 viroporin structure

Benjamin P. Oestringer†‡, Juan H. Bolivar†‡, Mario Hensen†‡, Jolyon K. Claridge†§, Chris Chipot‖¶, François Dehez‖, Nicole Holzmann‖, Nicole Zitzmann†‡* & Jason R. Schnell†*

† Department of Biochemistry, University of Oxford, South Parks Road, Oxford OX1 3QU, United Kingdom

‡ Oxford Glycobiology Institute, Department of Biochemistry, University of Oxford, South Parks Road, Oxford, OX1 3QU, United Kingdom.

‖ Laboratoire International Associé CNRS-University of Illinois at Urbana Champaign, Université de Lorraine, BP 70239, 54506 Vandœuvre-lès-Nancy, France

¶ Department of Physics, University of Illinois at Urbana-Champaign, 1110 West Green Street, Urbana, Illinois 61801, United States

ARISING FROM B. OuYang *et al*. *Nature* **498**, 521–525 (2013); doi: 10.1038/nature12283

The Hepatitis C virus (HCV) p7 viroporin is a membrane protein required for virus propagation *in vivo* that assembles into hexamers and heptamers in membranes, exhibits ion channel activity, and is an attractive target against HCV infection[1]. OuYang and colleagues reported an oligomeric structure of p7 with unexpected features, solubilized in dodecylphosphocholine (DPC) detergent.[2] We show that p7 is monomeric in the conditions employed to determine its oligomeric structure and that the data presented as evidence for intermolecular contacts most likely arises from incomplete protein deuteration. We conclude that p7 is monomeric under NMR conditions and that the oligomeric structure proposed by OuYang *et al*. is artefactual.

Unexpected features of the p7 oligomeric structure include: (i) the His17 sidechain, known to be involved in ion conduction[3,4], points outward toward the membrane bilayer, (ii) the oligomeric structure fits best to the electron microscopy (EM) envelope in an orientation contradicting antibody binding data[5], and (iii) a short outer transmembrane helix exposes polar residues to the hydrophobic region of the membrane so that the structure cannot be accommodated in lipid bilayers without large structural rearrangements or membrane thinning[6,7] (**Extended Data Figure 1AB**).

We expressed, purified, and reconstituted into DPC ^{15}N-labelled protein corresponding to the genotype 5a isolate EUH1480 p7 protein containing five amino acid substitutions (p7(5a/EUH1480)mut) as described.[2] Overlays of backbone ^{1}H,^{15}N correlation NMR spectra confirm that the solution conditions and protein conformation are similar to those studied previously (**Extended Data Figure 2A**).[2,8] High quality backbone spectra of fully protonated p7 in DPC could be recorded at 37˚C using conventional, HSQC-based experiments (**Extended Data Figure 2B**), which is unexpected for a protein complex of 60-80 kDa (protein oligomer plus associated detergent micelle).[9] The spectra were unchanged between 30˚C and 37˚C, indicating that the protein adopted a similar conformation over this temperature range (**Extended Data Figure 2C**).

Two methods were used to obtain information on the size of the p7 and detergent micelle complex. First, we estimated the effective protein mass using the rotational correlation time derived from ^{15}N R_1 and R_2 relaxation rates. The rotational correlation time, 10.1 ns at 37˚C, corresponds to 39.3 kDa, similar to a hexameric p7 (~41 kDa) in the absence of a detergent micelle. Alternatively, the same rotational correlation time corresponds to monomeric p7 and a micelle of ~70 detergent molecules. We then applied size-exclusion chromatography coupled to multi-angle light scattering (SEC-MALS), which decomposes masses into protein and detergent contributions and is reliable for proteins like p7, having a high molar extinction coefficient (17,990 M^{-1} cm^{-1}) and a relatively high light scattering intensity due to the detergent micelle.[10] P7 samples reconstituted according to OuYang *et al.* and loaded onto SEC-MALS in conditions similar to those used for NMR studies (50 mM DPC; **Figure 1A**) or EM studies (3 mM DPC but at higher protein concentration; **Figure 1B**) indicated protein masses consistent with monomers (6.4 ± 1.1 kDa and 8.4 ± 0.7 kDa, respectively) associated with detergent micelles of 23.5 ± 0.5 kDa and 42.4 ± 3.7 kDa, respectively (**Extended Data Table 1**). A third sample prepared according to Dev *et al*. (50 mM DPC)[8], indicated a protein mass of 7.8 ± 1.1 kDa associated with a detergent micelle of 24.7 ± 0.6 kDa (**Extended Data Figure 3A**). Moreover, NMR spectra matching exactly the protein and detergent concentrations at the monomeric SEC-MALS peak summit (5 µM protein and 50 mM DPC) overlay well with the spectrum published by OuYang *et al*. (**Extended Data Figure 2D**).

The SEC-MALS results are confirmed by comparison with p7 solubilized in sodium dodecyl sulfate (SDS) at “low” (<2 times the critical micelle concentration (CMC)) and “high” (≥10 times the CMC) detergent concentrations. SDS is strongly denaturing and p7 runs as a monomer on SDS-PAGE.[2] Results for p7 in high (80 mM) and low (10 mM)

SDS concentrations are consistent with a monomer, as expected, and similar to the results with DPC in that low concentrations of SDS lead to an increase in detergent micelle size with no change in oligomerization state (**Extended Data Figures 3B-E** and **Extended Data Table 1**). The same trend in micelle size with detergent concentration, though less marked, is observed in the absence of protein (**Extended Data Figure 3F-I** and **Extended Data Table 2**).

OuYang *et al.* identified putative intermolecular NOEs (nuclear Overhauser effects) from a 3D ^{15}N-edited NOESY-TROSY experiment, without filtering for ^{13}C-attached protons, on a sample containing a 1:1 mixture of ^{15}N/^{2}H- and ^{13}C-labelled proteins. This experiment can provide intermolecular NOEs between exchangeable amide protons of the ^{15}N/^{2}H-labelled protein and non-exchangeable aliphatic protons of the ^{13}C-labelled protein. Artefactual cross-peaks can arise from incomplete deuteration of the ^{15}N/^{2}H-labelled protein, and a control NOESY experiment must be recorded on an unmixed but otherwise identical sample of ^{15}N/^{2}H-labelled protein since commercial sources of D_2O and deuterated glucose contain at least small amounts of protons and additional protons can be carried over from starter cultures and humidity in the air. Control experiments were not reported by OuYang *et al.*, but comparison of the mixed label NOESY with a NOESY collected on fully protonated protein can indicate whether the NOEs are consistent with trace protonation of the ^{15}N/^{2}H-labelled protein. The NOESY spectra were aligned in the indirect ^{1}H dimensions such that the amide proton chemical shifts, which have relatively small deuterium isotope shifts, were consistent. Seven NOEs were identified by OuYang *et al.* as unambiguously intermolecular, and for each of these that could be identified in their mixed label NOESY spectrum there is a corresponding strong peak in their fully protonated sample NOESY close to the position expected for an intra-residue proton (**Figure 2A**). The mixed label NOEs were slightly up-field shifted on the order of 0.01 ppm, consistent with the deuterium isotope shifts expected for protons in a mostly deuterated background (*e.g.*, as –C^{2}H$_2$^{1}H in methyls). The deuterium shift can be large enough (~0.04 ppm in alanine methyls[11]) to result in misinterpretation of NOEs as long-range. Of the 58 observable backbone amides in p7, at least 18 (31%) exhibit NOEs consistent with residual protonation (**Figure 2A**). In addition, the observed crosspeaks tend to correlate with sidechain protons closer to the backbone. Alanines should be most susceptible to NOE artefacts from trace protonation since the methyls are close to the backbone amide proton and the three deuterium positions increase the probability of a proton being present. Indeed, six of eight assigned alanines show crosspeaks in the mixed label sample that correlate with the intramolecular Hβ chemical shift.

NOE crosspeaks assigned to intermolecular interactions with rimantadine in an ^{15}N/^{2}H-labelled sample containing 5 mM rimantadine are also consistent with trace protonation since those peaks are present in the rimantadine-free mixed label sample, and those crosspeaks correlate with intra-residue sidechain protons (**Figure 2B**). Similar cross-peaks are also attributed to an amantadine interaction.[2] Among valine, leucine, and isoleucine methyls, OuYang *et al.* reported large methyl chemical shift perturbations upon addition of rimantadine for Val7-γ2, Val25-γ2, and Val53-γ1 methyls, of which only Val25 and Val53 are near the proposed binding site. To provide greater data coverage, we used the backbone amide spectra of OuYang *et al*. to calculate chemical shift differences upon addition of 5 mM rimantadine. A large number of residues across the protein exhibit chemical shift differences in an apparently nonspecific manner (**Extended Data Figure 2E**), and residues identified as lining the rimantadine and amantadine binding site (Fig. 3c of OuYang *et al.*) show some of the smallest chemical shift differences. The distribution and magnitude of the shifts are similar to what was observed after addition of amantadine to a sample of monomeric p7 at pH 4.0 and 50˚C.[12] The rimantadine K_d values reported by OuYang *et al.* (13.2 μM and 63.6 μM) are at least three orders of magnitude higher than for the equivalent values in membranes[13], and are consistent with nonspecific binding.

OuYang *et al.* used residual dipolar couplings (RDCs) to calculate their p7 structure. Although RDCs do not directly report on oligomer stoichiometry, best fits of their RDC data to the deposited structures result in alignment tensors with large, nonzero rhombicities (>0.48; average of 0.57) which are inconsistent with a tightly associated, symmetric oligomer.[14] We note also that refinement against a single set of amide bond RDCs from one alignment medium will not yield a unique structure in the absence of information about long-range contacts.[15] This means that it is possible to fit the amide bond RDCs to a p7 subunit structure influenced by incorrectly assigned intermolecular restraints.

In conclusion, we find that p7 is monomeric over a range of protein and DPC concentrations, including the NMR conditions reported by OuYang *et al.* to determine an oligomeric structure, and that NOEs identified as unambiguously intermolecular are consistent with artefacts from residual protonation. We note that the protein concentration (200 nM monomer) used in the EM experiments cannot be analyzed by NMR or SEC-MALS, hence oligomerization upon sample dilution for EM studies cannot be ruled out. Moreover, it cannot be excluded that the p7 oligomeric complexes observed by EM represent a small proportion of the total protein sample not detectable by NMR or SEC-MALS.

Methods

Estimation of complex size from NMR relaxation data. To exclude data from residues with internal motions faster or slower than the overall tumbling time, the τ_c was calculated from the 20% trimmed means of the ^{15}N relaxation rates[16], which were 1.34 s^{-1} and 14.80 s^{-1} for R_1 and R_2, respectively. ^{15}N relaxation rates were measured using HSQC-based experiments. The molecular weight was calculated from τ_c using Stoke's law assuming a hydration shell of 1.5 water molecules, a solution viscosity of 0.702 centipoise at 37˚C, and a protein partial specific volume of 0.73 cm^3/g. The different partial specific volumes of protein (0.73 cm^3/g) and micellar DPC (0.94 cm^3/g) were taken into account to calculate the number of attached detergent molecules.

SEC-MALS. SEC-MALS was performed on a Shimadzu Nexera HPLC and a MALS DAWN HELEOS II and a refractive index Optilab T-rEX detector (Wyatt Technology). Determination of the molar masses was performed using protein conjugate analysis. A dn/dc value of 0.1398 ml/g was used for DPC (Anatrace). A dn/dc value of 0.1100 ml/g was used for SDS.[17] For detergent alone samples, micelle molar masses were determined by the standard analysis tool in Astra 6.1.1.17 based on light scattering and refractive index.

Data Availability

All data are available on request from the corresponding authors.

ASSOCIATED CONTENT

Supplementary Information

AUTHOR INFORMATION

Corresponding Authors

†* Department of Biochemistry, University of Oxford, South Parks Road, Oxford OX1 3QU, United Kingdom. Electronic address: Jason.Schnell@bioch.ox.ac.uk

†‡* Oxford Glycobiology Institute, Department of Biochemistry, University of Oxford, South Parks Road, Oxford, OX1 3QU, United Kingdom. Electronic address: Nicole.Zitzmann@bioch.ox.ac.uk

Present Addresses

†‡ Immunocore Limited, 101 Park Drive, Milton Park, Abingdon, Oxon, OX14 4RY, United Kingdom

†§ Structural Biology Brussels, Vrije Universiteit Brussel, Pleinlaan 2, 1050 Brussels, Belgium, and Structural and Molecular Microbiology, Structural Biology Research Center, VIB, Pleinlaan 2, 1050 Brussels, Belgium

Competing financial interests

The authors declare no competing financial interests.

Author contributions

B.P.O. performed protein expression, sample preparation, NMR experiments and data analysis, SEC-MALS experiments and analysis and helped write the paper; J.H.B. performed sample preparation, SEC-MALS experiments and analysis and helped write the paper; M.H. performed protein expression, sample preparation and SEC-MALS experiments; J.K.C. performed NMR experiments and data analysis; C.C., F.D. and N.H. performed MD; J.R.S. performed NMR experiments and reanalyzed NOESY spectra; N.Z. performed protein expression and sample preparation; J.R.S., N.Z., C.C. and F.D. conceived the study; J.R.S. and N.Z. wrote the paper.

Acknowledgements

We thank Prof. Christina Redfield for discussions about NMR data analyses.

Figure Legends

Figure 1. SEC-MALS of p7 in 3 mM and 50 mM DPC. Left axis: UV, absorbance at 280 nm; LS, light scattering; RI, refractive index. Right axis: molar masses calculated at each point for protein, associated detergent and the detergent and protein complex. Insets show the three detector signals normalized at the p7 peak. The DPC concentration and maximum p7 monomeric concentration eluted (summit of peak) are indicated on the graphs. Reported masses denote the value at the peak summit and the error is taken as the maximum difference to this value across the elution volume for which the molar mass is plotted. A summary of all SEC-MALS conditions and calculated masses is in **Table S1**. **(A)** SEC-MALS of a sample resembling NMR conditions used to calculate the putative hexameric structure.[2] The protein was dissolved into 200 mM DPC and 6 M guanidine and reconstituted by dialysis as described,[2,8] with a final DPC concentration of 50 mM. A 50 mM DPC concentration[8] was chosen instead of 200 mM[2] because the scattering intensity at 200 mM DPC saturates the detector. A Superdex 200 10/300 column was used. The calculated mass values were 6.4 ± 1.1 kDa for the protein and 23.5 ± 0.5 kDa for the associated detergent. **(B)** Sample prepared as for EM studies[2] (3 mM DPC), but at higher protein concentration. P7 was refolded in 200 mM DPC, then run over SEC on a Superdex 200 10/300 column in 3 mM DPC to remove excess DPC. A small amount of protein aggregates with large scattering and refractive index peaks were observed before the monomeric p7 peak (similar to those seen in **(A)**). The p7 monodisperse peak was collected and analyzed by SEC-MALS with 3 mM DPC running buffer in a Superdex 200 5/150. The calculated molar masses were 8.4 ± 0.7 and 42.4 ± 3.7 kDa for protein and the associated detergent, respectively.

Figure 2: Evidence of residual protonation from comparison of 3D ^{15}N-edited NOESY strips. (A) Alignments of indirect ^{1}H dimension strips from the 3D ^{15}N-edited NOESY spectra of OuYang *et al.* are shown. For each residue indicated at the top, the left strip is from the mixed label sample (1:1 mixture of ^{15}N/^{2}H- and ^{13}C-labelled p7) and the right strip is from a ^{15}N/^{1}H-labelled sample. Positive contours are in black and negative contours in grey. Horizontal red dashed lines are added to show chemical shift correlations between strips and are positioned at the chemical shifts of selected intra-molecular NOEs in the fully protonated sample. Asterisks indicate strips from which putative intermolecular NOEs were identified by OuYang *et al.*: Ile6 H_N (to Ile6 $H_{\gamma 2}$), Val7 H_N (to Val5 $H_{\gamma 1}$), Ala11 H_N (to Ala61 H_β), Ala14 H_N (to Ala63 H_β), Leu23 H_N (to Ala29 H_β), and Leu24 H_N (to Ala29 H_β). The positions of the putative intermolecular NOEs correlate well with positions of strong intra-residue peaks in the fully protonated sample: Ile6 H_N (to Ile6 $H_{\gamma 2}$), Val7 H_N (to Val7 $H_{\gamma 1}$), Ala11 H_N (to Ala11 H_β), Ala14 H_N (to Ala14 H_β), Leu23 H_N (to Leu23 H_β), and Leu24 H_N (to Leu24 H_β). Several strips from the mixed label NOESY indicate more than one correlation to an intra-residue NOE in the fully protonated sample. For the putative intermolecular NOE at Gly15 H_N (to His59 $H_{\varepsilon 1}$), no obvious, resolvable crosspeaks corresponding to His59 sidechain protons were identifiable in the mixed label NOESY, however, trace protonation at the Gly15 $H\alpha$ is apparent in the mixed label NOESY strip. Diagrams showing the strip for this NOE were not presented in the supplementary information of OuYang *et al.* An eighth NOE not present in the restraint file deposited with the BMRB but indicated in the OuYang *et al.* paper (supplementary Figure 8) is from Ala10 (H_N) to Ala61 ($H\beta$), which also can be explained as an intra-molecular NOE arising from trace protonation. **(B)** Analysis of putative intermolecular NOEs to rimantadine. For each residue indicated at top, the left and middle strips correspond to the NOESYs shown in **(A)**, and the additional strip on the right is from a ^{15}N/^{2}H-labelled sample containing 5 mM rimantadine. NOEs identified by OuYang *et al.* as arising from rimantadine (see also supplementary Figure 6 of OuYang *et al.*) correlate with intra-molecular NOEs observed for the fully protonated sample and for the mixed label sample, both of which have no rimantadine added.

REFERENCES

1. Madan, V. & Bartenschlager, R. Structural and functional properties of the Hepatitis C Virus p7 viroporin. *Viruses* **7,** 4461–4481 (2015).
2. OuYang, B. *et al.* Unusual architecture of the p7 channel from hepatitis C virus. *Nature* **498,** 521–525 (2013).
3. Chew, C. F., Vijayan, R., Chang, J., Zitzmann, N. & Biggin, P. C. Determination of pore-lining residues in the hepatitis C virus p7 protein. *Biophysical journal* **96,** L10–2 (2009).
4. Stgelais, C. *et al.* Determinants of hepatitis C virus p7 ion channel function and drug sensitivity identified in vitro. *Journal of virology* **83,** 7970–7981 (2009).
5. Luik, P. *et al.* The 3-dimensional structure of a hepatitis C virus p7 ion channel by electron microscopy. *Proceedings of the National Academy of Sciences of the United States of America* **106,** 12712–12716 (2009).
6. Stansfeld, P. J. *et al.* MemProtMD: Automated Insertion of Membrane Protein Structures into Explicit Lipid Membranes. *Structure* **23,** 1350–1361 (2015).
7. Kalita, M. M., Griffin, S., Chou, J. J. & Fischer, W. B. Genotype-specific differences in structural features of hepatitis C virus (HCV) p7 membrane protein. *Biochimica et biophysica acta* **1848,** 1383–1392 (2015).
8. Dev, J., Brüschweiler, S., OuYang, B. & Chou, J. J. Transverse relaxation dispersion of the p7 membrane channel from hepatitis C virus reveals conformational breathing. *J. Biomol. NMR* **61,** 369–378 (2015).
9. Fernández, C. & Wider, G. TROSY in NMR studies of the structure and function of large biological macromolecules. *Current opinion in structural biology* **13,** 570–580 (2003).
10. Korepanova, A. & Matayoshi, E. D. HPLC-SEC characterization of membrane protein-detergent complexes. *Curr Protoc Protein Sci* **Chapter 29,** Unit 29.5.1–12 (2012).
11. Gardner, K. H., Rosen, M. K. & Kay, L. E. Global folds of highly deuterated, methyl-protonated proteins by multidimensional NMR. *Biochemistry* **36,** 1389–1401 (1997).
12. Cook, G. A., Dawson, L. A., Tian, Y. & Opella, S. J. Three-dimensional structure and interaction studies of hepatitis C virus p7 in 1,2-dihexanoyl-sn-glycero-3-phosphocholine by solution nuclear magnetic resonance. *Biochemistry* **52,** 5295–5303 (2013).
13. Breitinger, U., Farag, N. S., Ali, N. K. M. & Breitinger, H.-G. A. Patch-Clamp Study of Hepatitis C p7 Channels Reveals Genotype-Specific Sensitivity to Inhibitors. *Biophysical journal* **110,** 2419–2429 (2016).
14. Al-Hashimi, H. M., Bolon, P. J. & Prestegard, J. H. Molecular symmetry as an aid to geometry determination in ligand protein complexes. *J. Magn. Reson.* **142,** 153–158 (2000).
15. Hus, J.-C. *et al.* 16-fold degeneracy of peptide plane orientations from residual dipolar couplings: analytical treatment and implications for protein structure determination. *J. Am. Chem. Soc.* **130,** 15927–15937 (2008).
16. Kay, L. E., Torchia, D. A. & Bax, A. Backbone dynamics of proteins as studied by nitrogen-15 inverse detected heteronuclear NMR spectroscopy: application to staphylococcal nuclease. *Biochemistry* (1989).
17. Tumolo, T., Angnes, L. & Baptista, M. S. Determination of the refractive index increment (dn/dc) of molecule and macromolecule solutions by surface plasmon resonance. *Anal. Biochem.* **333,** 273–279 (2004).

Extended Data

Extended Data Table 1: Summary of conditions and results for SEC-MALS studies of p7(5a/EUH1480)mut in DPC and SDS. Data from **Extended Data Figures 2B and Extended Data 2C** show that at similar detergent/protein molar ratios the molar mass of detergent associated to p7 is approximately double in 10 mM SDS compared to p7 in 80 mM SDS. Data from **Extended Data Figure 2D and Extended Data Figure 2E** show that the result is consistent when changing the protein concentration. Together with the data in DPC (**Figure 1**), the results suggest that at detergent concentrations close to the CMC (~8 mM for SDS and ~1.5 mM for DPC) a larger number of detergent molecules associate with p7. Running buffers contained the indicated detergent concentrations and 25 mM MES at pH 6.5 (DPC samples) or 10 mM sodium phosphate at pH 7.2 (SDS samples). The chromatography columns were Superdex 200 of sizes 10/300 (**Figure 1A**) and 5/150 (**Figure 1B**) or two 5/150 columns attached in series (**Figures 2A-E**), depending on sample volumes and concentrations and resolution requirements. The samples pre-injection contained the same detergent concentration as the running buffer. Reported masses denote the value at the peak summit and the error is taken as the maximum difference to this value across the elution volume for which the molar mass is plotted in the SEC-MALS figures.

Extended Data Table 2: Summary of conditions and results for SEC-MALS studies of DPC and SDS detergents in the absence of protein. Data is from experiments shown in **Extended Data Figures 2F-I**. The micelle molar masses calculated from the SEC-MALS data at concentrations close to the CMC (~8 mM for SDS and ~1.5 mM for DPC) are in close agreement with those reported in the literature: ~19.0 kDa for DPC (Anatrace measurement in collaboration with Prof. Mark Foster, University of Akron) and ~17.3 kDa for SDS.[1] At the higher detergent concentrations, the micelle molar masses decrease by ~3 kDa for DPC and ~10 kDa for SDS. Running buffers contained the indicated detergent concentrations and 25 mM MES at pH 6.5 (DPC samples) or 10 mM sodium phosphate at pH 7.2 (SDS samples). Reported masses denote the value at the peak summit and the error is taken as the maximum difference to this value across the elution volume for which the molar mass is shown in the SEC-MALS figures.

Extended Data Figure 1: Molecular Dynamics of p7(5a/EUH1480)mut. (**A**)-(**B**) Insertion of the hexameric p7 structure of OuYang *et al.*[2] into lipid bilayers. (**A**) MemProtMD[3] prediction for the hexamer insertion into a hydrated 1,2-dipalmitoyl-*sn*-glycero-3-phosphatidylcholine (DPPC) bilayer. (**B**) The p7 structure of OuYang *et al*.[1] after insertion into a hydrated 1-palmitoyl-2-oleoyl-*sn*-glycero-3-phosphatidylcholine (POPC) bilayer and simulated for 60 ns. Severe deformations and thinning defects of the bilayer can be seen, resulting in a large number of water molecules within the hydrophobic region of the bilayer. Water is shown as van der Waals spheres for oxygen (red) and hydrogen (white). For DPPC and POPC lipids, phosphorus and choline nitrogen positions are indicated with orange spheres and green spheres, respectively. (**C**)-(**E**) Simulations of monomeric p7 in 300 mM DPC at a ratio of protein to detergent of 1:250. In (**C**) and (**D**) are shown two independent 100 ns simulations of the horseshoe-like subunit conformation of the OuYang *et al*. structure. At the end of the simulation, ~170 and ~120 DPC molecules, respectively, were observed bound to the protein. In (**E**), a hairpin conformation of p7(5a/EUH1480)mut was simulated for 100 ns, at the end of which ~100 DPC molecules were observed bound to the protein. In (**C**)-(**E**), p7 α-helices and 3_{10} helices are shown in magenta and blue, respectively, the geometric center of the DPC headgroup is indicated by an orange sphere, and the DPC hydrocarbon chain as yellow sticks. Only those DPC molecules bound to p7 are shown. The simulations in (**B**)-(**E**) were performed with CHARMM36 all-atom force field using the protocol described previously.[4]

Extended Data Figure 2: NMR spectroscopy of p7(5a/EUH1480)mut in DPC. All reported concentrations are for monomeric protein. **(A)** Comparison of the p7(5a/EUH1480)mut prepared according to OuYang *et al*. with previously published spectra. Left: 2D ^{1}H,^{15}N TROSY spectrum of a p7(5a/EUH1480)mut sample in DPC produced in this study (red crosspeaks) recorded at 30˚C and a ^{1}H frequency of 600 MHz overlayed with the spectrum published in OuYang *et al.* (blue crosspeaks).[2] Right: our p7(5a/EUH1480)mut spectrum (red crosspeaks) overlayed with the spectrum presented in Dev *et al.* (2015) (blue crosspeaks)[5] to illustrate sample to sample variation. In both cases the spectra were overlayed manually. (**B**) ^{1}H,^{15}N HSQC of p7(5a/EUH1480)mut in DPC at 37˚C. The spectrum was recorded at 600 MHz (^{1}H) on a Bruker spectrometer equipped with a CryoProbe. **(C)** Temperature sensitivity of the p7(5a/EUH1480)mut spectrum in DPC. Spectra were recorded at three temperatures: 30°C (blue), 33.5°C (green) and 37°C (red). The spectra have not been corrected for the temperature dependence of the ^{2}H lock frequency. **(D)** NMR spectra of p7(5a/EUH1480)mut under SEC-MALS conditions. Spectra were recorded of p7(5a/EUH1480)mut at 5 µM protein and 50 mM DPC (detergent-to-protein ratio of 10,000) to match conditions at the SEC-MALS peak summit for a sample prepared as described in OuYang *et al.*[2] (violet) (see **Figure 1A** and **Extended Data Table 1**), or as described in Dev *et al*.[5] with pre-gel filtration in 3 mM DPC buffer containing 100 mM NaCl (orange) (see **Extended Data Figure 3A**). Before recording the NMR data, the Dev *et al*. sample was dialysed against buffer (25 mM MES at pH 6.5, 3 mM DPC, and 1 mM DSS with 5% D_2O) overnight to remove salt, concentrated, and then diluted with NMR buffer (25 mM MES at pH 6.5, 50 mM DPC, and 1 mM DSS with 5% D_2O)

to match the concentrations at the peak summit of the SEC-MALS elution (5 µM peptide and 50 mM DPC). BEST-TROSY NMR experiments were recorded over ~20 hours each on a 750 MHz spectrometer equipped with a CryoProbe to obtain sufficient signal-to-noise on the dilute samples and overlaid with the published TROSY spectra (Supplementary Figure 2A of OuYang *et al*.). **(E)** Backbone amide chemical shift differences between a sample of p7(5a/EUH1480)mut in DPC without and with 5 mM rimantadine. Data analysis was carried out on the spectra of OuYang *et al*. Chemical shift differences were calculated as indicated on the vertical axis for the backbone amide resonances in the $^{15}N/^{2}H$-labelled mixed label sample and the $^{15}N/^{2}H$-labelled sample containing 5 mM rimantadine. Residues in pink were identified by OuYang *et al*. as forming the rimantadine binding pocket (see Figure 3c of OuYang *et al*.).

Extended Data Figure 3: SEC-MALS of p7(5a/EUH1480)mut and detergent alone. The right axes denote the molar masses calculated at each point for protein (Prot; if protein is present), associated detergent (Det), and the detergent and protein complex (Det + Prot; if protein is present). The left axes show the three detector signals UV (absorbance 280 nm; if protein is present), LS (light scattering) and RI (refractive index). Detector signals are scaled to allow for comparison. In (A), the inset shows the detector signals normalized at the p7(5a/EUH1480)mut peak. A summary of experimental conditions and mass calculations are in **Extended Data Table 1** and **Extended Data Table 2**. The reported masses denote the value at the peak summit and the error is taken as the maximum difference to this value across the elution volume for which the molar mass is plotted. For samples with p7, negative and positive scattering and refractive index peaks following the protein peaks are the result of distortions of the baseline upon sample injection that causes disequilibrium of detergent micelles in the running buffer.[6] **(A)** P7 in 50 mM DPC prepared as described by Dev. *et al.* The sample was run over two Superdex 200 5/150 columns in series in order to resolve the protein and micelle complex. The calculated masses were 7.8 ± 1.1 and 24.7 ± 0.6 kDa for protein and the associated detergent, respectively. The DPC concentration and maximum p7 monomeric concentration eluted (summit of peak) are indicated above the graph. **(B)-(E)** SEC-MALS of p7(5a/EUH1480)mut in 80 mM and 10 mM SDS. The SDS concentration and the maximum p7 monomeric concentration eluted (summit of peak) are indicated above each graph. P7 is monomeric in SDS, as evidenced by its mobility on SDS-PAGE (OuYang *et al*. and our data not shown). SEC-MALS molar mass analysis indicates unambiguously a monomeric state for p7 in SDS in all cases. The analysis also confirms the trend seen with DPC (**Figures 1** and **(A)** above), in that the amount of detergent associated with the protein is markedly and consistently higher for the samples at the lower detergent concentration (10 mM SDS) compared with samples in higher detergent concentration (80 mM SDS) (see data summary in **Extended Data Table 1**). Samples were run through two Superdex 200 5/150 columns connected in series for increased resolution. Sample injection volumes were 30 µl. Running buffer contained the indicated SDS concentrations and 10 mM sodium phosphate at pH 7.2. **(F)-(I):** SEC-MALS of DPC and SDS micelles in the absence of protein. The detergent, its concentration in the injected sample and running buffers, and the chromatography columns used are indicated above each graph. As in **(B)-(E)**, SDS samples were run over two Superdex 200 5/150 in series to increase resolution. The UV absorption at 280 nm in samples without protein is insignificant. Running buffers are the same as those used in experiments with protein (**Figure 1** and **(A)-(E)**), and the injected samples have higher detergent concentration to allow for detection above the baseline. In **(I)**, the running buffer contained 30 mM SDS because the smaller size micelles in 80 mM SDS in the absence of protein resulted in low signal-to-noise scattering. Molar masses (Det., orange line, right axis) increase slightly (by ~3 kDa for DPC and ~10 kDa for SDS) at concentrations close to their critical micelle concentration.

Extended Data References

1. Turro, N. J. & Yekta, A. Luminescent probes for detergent solutions. A simple procedure for determination of the mean aggregation number of micelles. J. Am. Chem. Soc. 100, 5951–5952 (1978).
2. OuYang, B. et al. Unusual architecture of the p7 channel from hepatitis C virus. Nature 498, 521–525 (2013).
3. Stansfeld, P. J. et al. MemProtMD: Automated Insertion of Membrane Protein Structures into Explicit Lipid Membranes. Structure 23, 1350–1361 (2015).
4. Holzmann, N., Chipot, C., Penin, F. & Dehez, F. Assessing the physiological relevance of alternate architectures of the p7 protein of hepatitis C virus in different environments. Bioorg. Med. Chem. (2016). doi:10.1016/j.bmc.2016.07.063
5. Dev, J., Brüschweiler, S., OuYang, B. & Chou, J. J. Transverse relaxation dispersion of the p7 membrane channel from hepatitis C virus reveals conformational breathing. J. Biomol. NMR 61, 369–378 (2015).
6. Slotboom, D. J., Duurkens, R. H., Olieman, K. & Erkens, G. B. Static light scattering to characterize membrane proteins in detergent solution. Methods 46, 73–82 (2008).

Figure 1

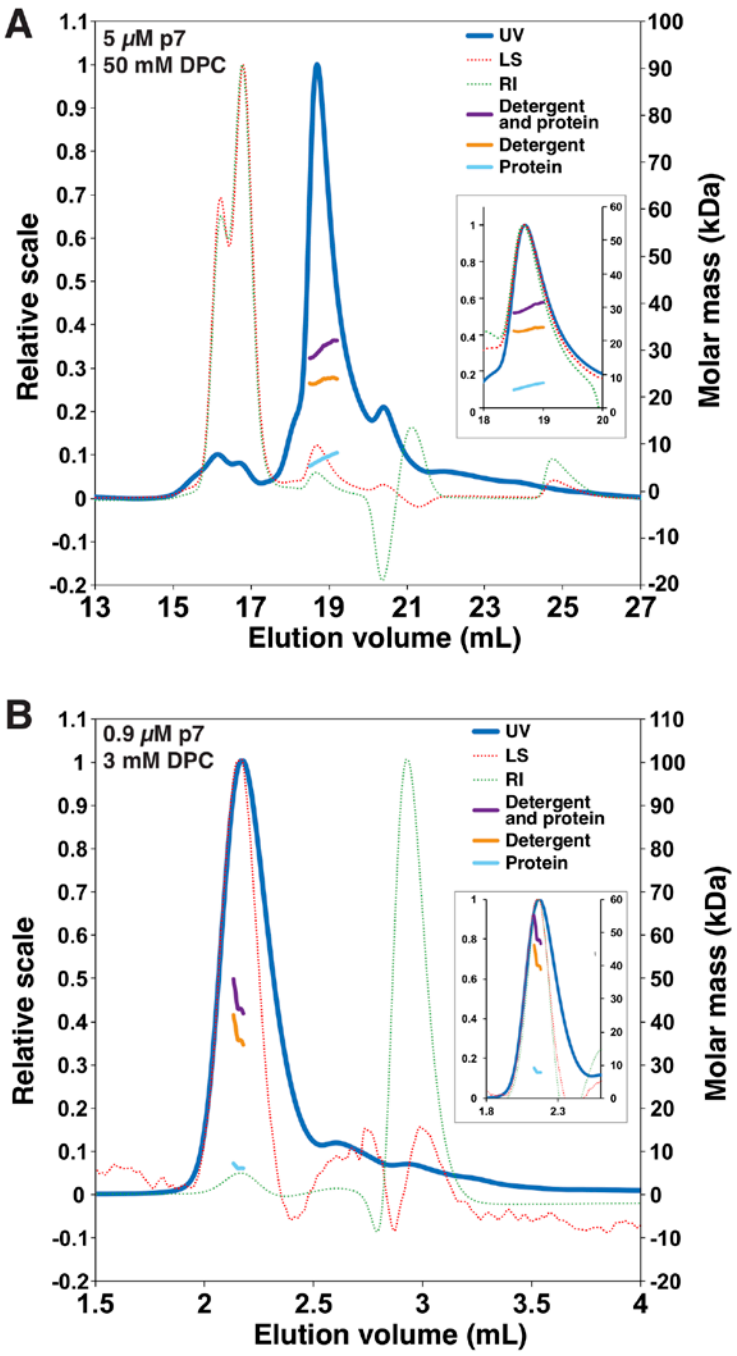
A
5 μM p7
50 mM DPC
UV
LS
RI
Detergent and protein
Detergent
Protein
Relative scale
Molar mass (kDa)
Elution volume (mL)
B
0.9 μM p7
3 mM DPC
UV
LS
RI
Detergent and protein
Detergent
Protein
Relative scale
Molar mass (kDa)
Elution volume (mL)

Figure 2

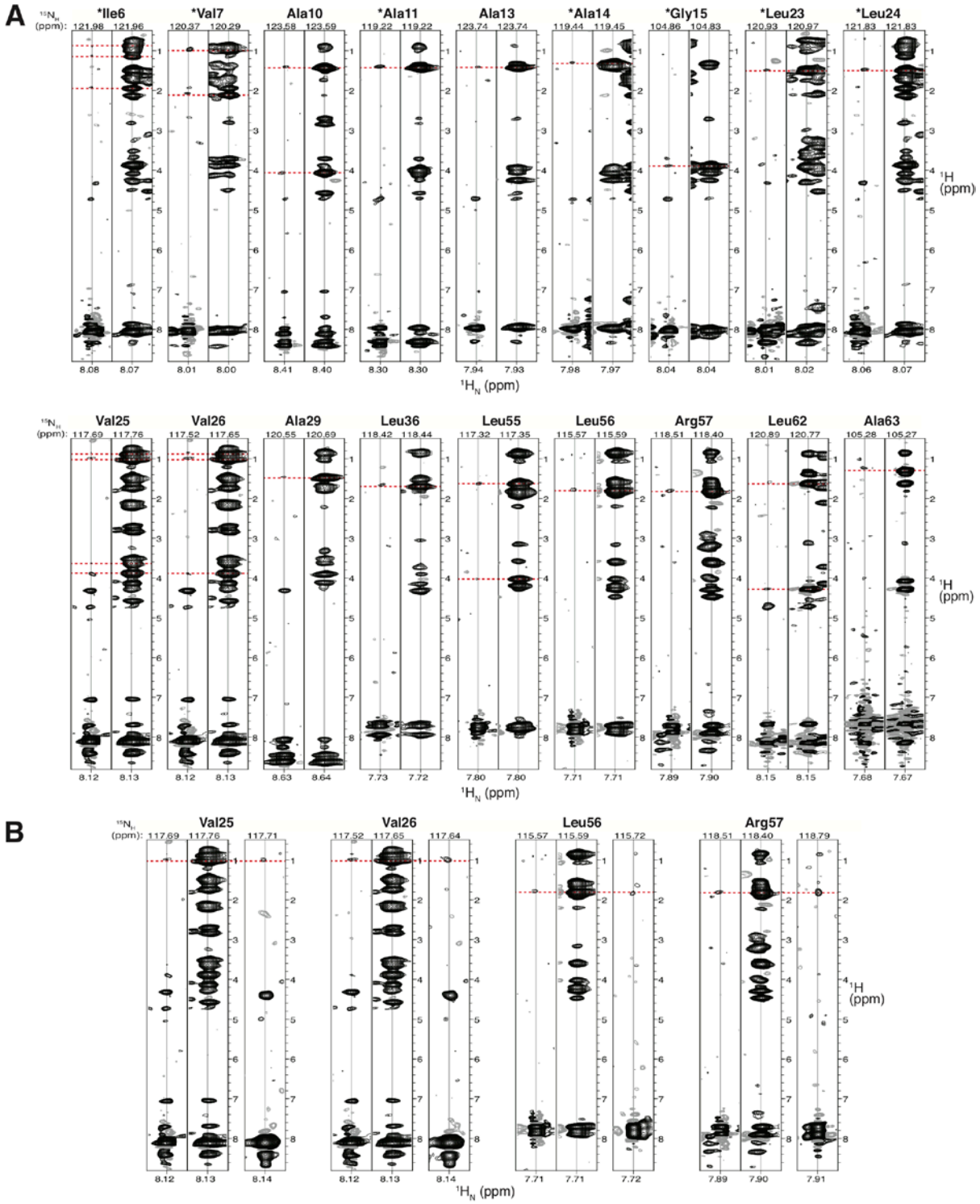
A
B
*Ile6
*Val7
Ala10
*Ala11
Ala13
*Ala14
*Gly15
*Leu23
*Leu24
Val25
Val26
Ala29
Leu36
Leu55
Leu56
Arg57
Leu62
Ala63
$^{15}N_H$ (ppm)
^1H_N (ppm)
^1H (ppm)

Extended Data Figure 1

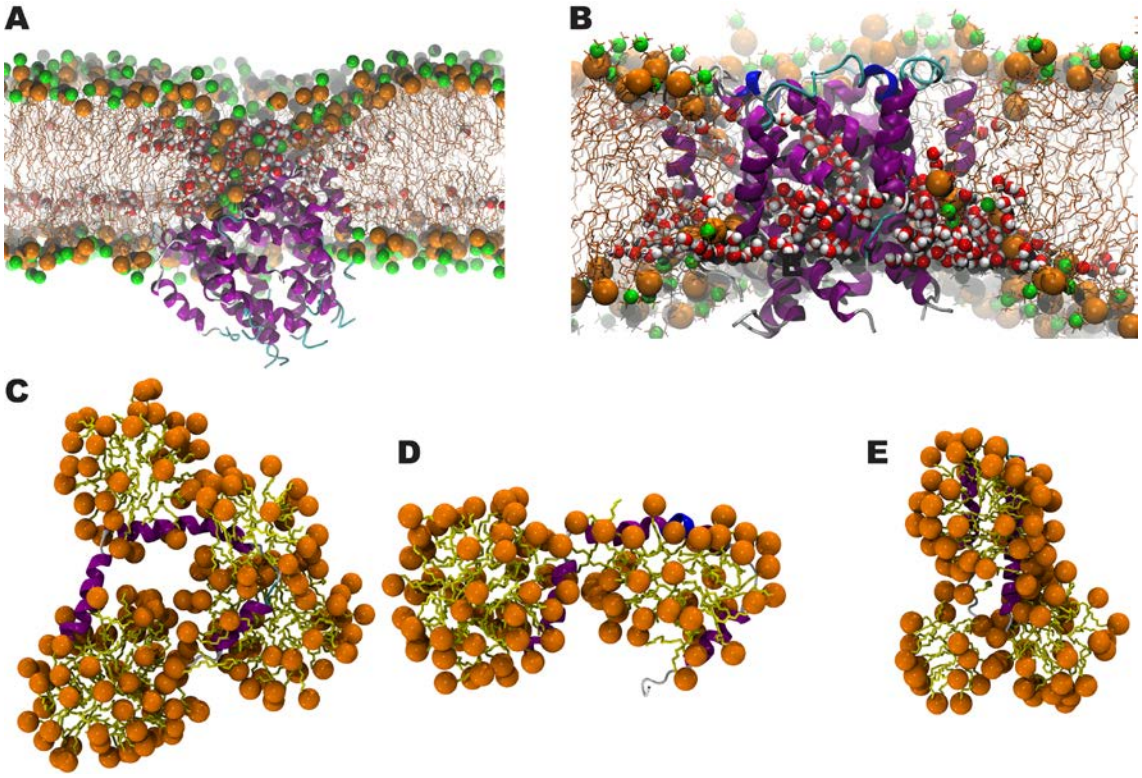

Extended Data Figure 2

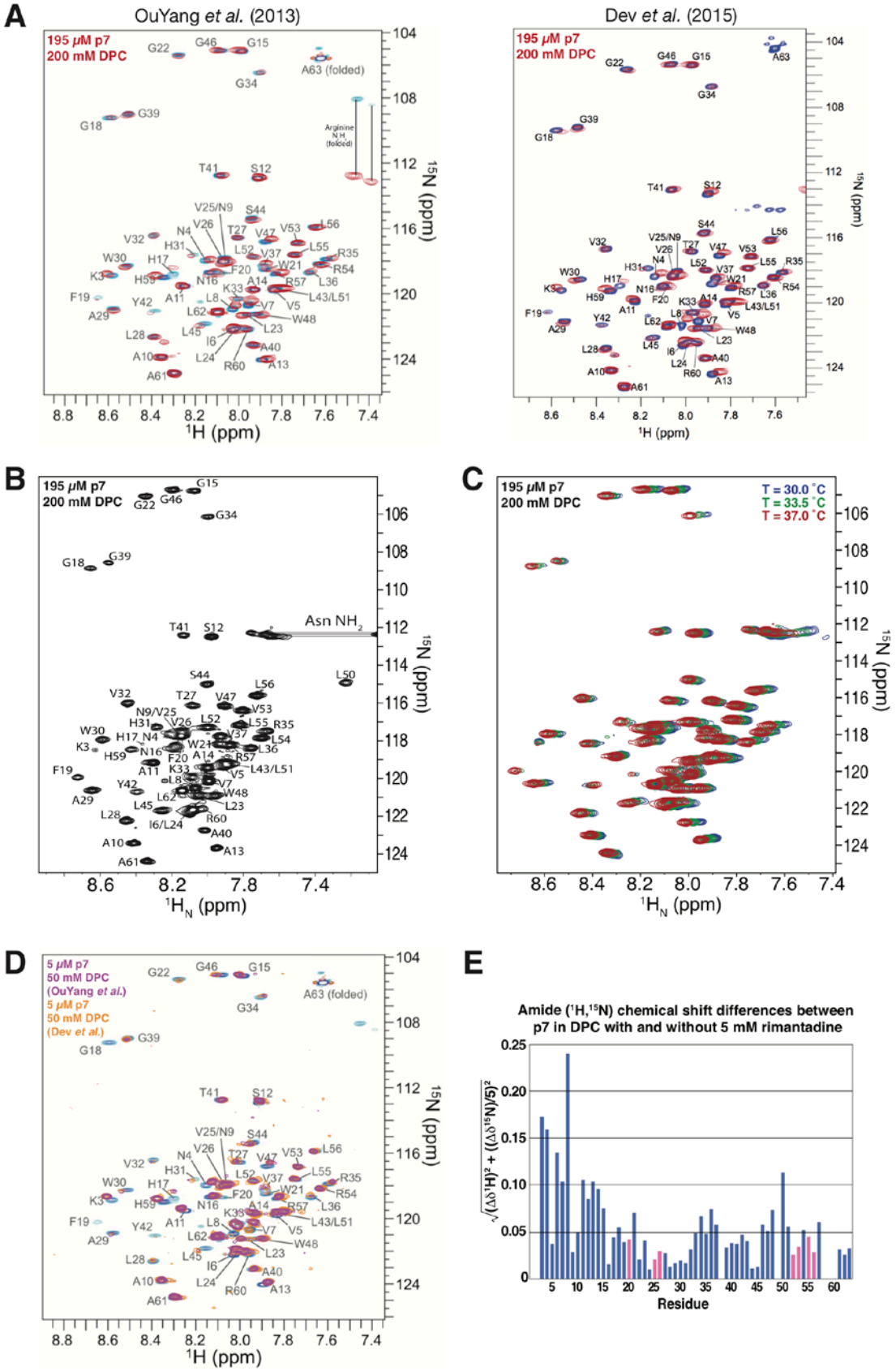

Extended Data Figure 3

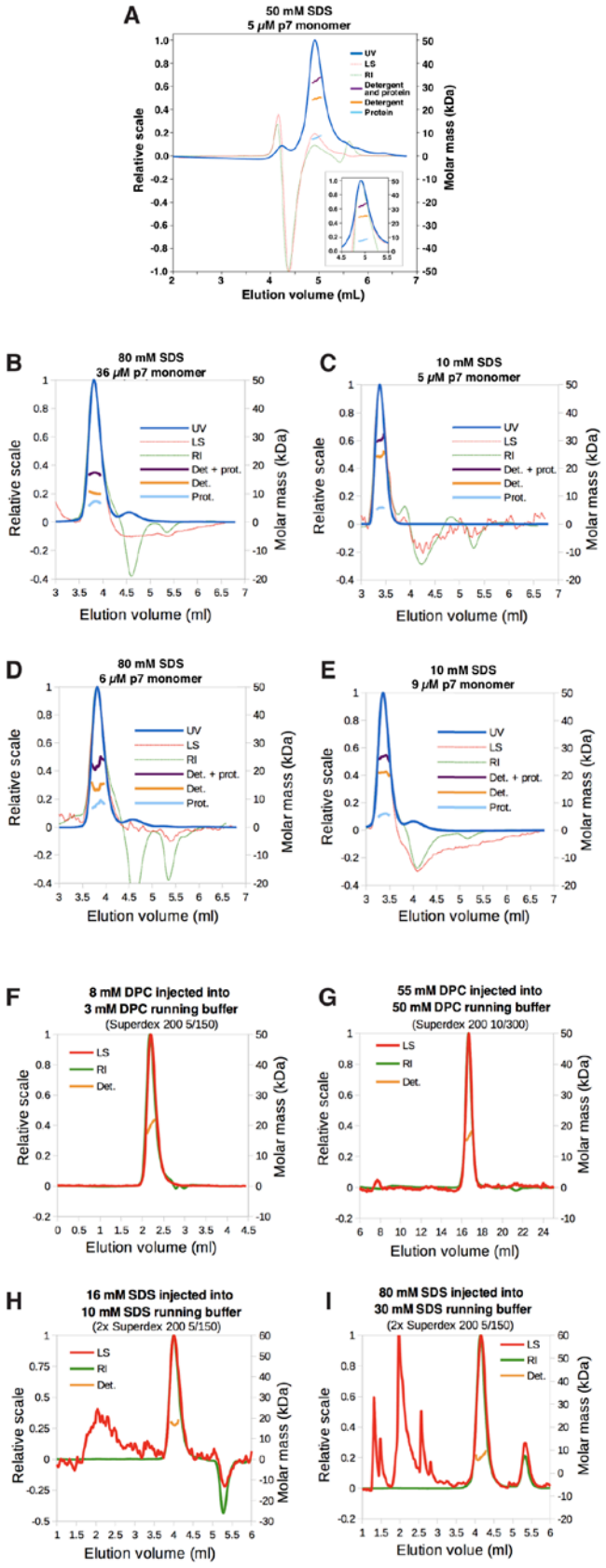

Extended Data Table 1

		Pre-injection			Eluted (peak summit)		Analysis of eluted p7 peak	
	Running buffer (mM)	p7 monomeric concentration (µM)	Det./Prot. (mol/mol)	Sample injection (µl)	p7 monomeric concentration (µM)	Det./Prot. (mol/mol)	Protein (kDa)	Detergent bound to p7 (kDa)
Fig 1A	50 mM DPC	200	250	70	5	10000	6.4 ± 1.1	23.5 ± 0.5
Fig 1B	3 mM DPC	15	200	15	0.9	3333	8.4 ± 0.7	42.4 ± 3.7
Ext. Data Fig 3A	50 mM DPC	140	357	50	5	10000	7.8 ± 1.1	24.7 ± 0.6
Ext. Data Fig 3B	80 mM SDS	464	172	30	36	2222	7.3 ± 1.8	10.2 ± 0.7
Ext. Data Fig 3C	10 mM SDS	58	172	30	5	2000	5.9 ± 0.8	24.1 ± 2.3
Ext. Data Fig 3D	80 mM SDS	58	1379	30	6	13333	8.3 ± 1.7	13.2 ± 3.1
Ext. Data Fig 3E	10 mM SDS	120	83	30	9	1111	5.9 ± 1.2	21.0 ± 1.5

Extended Data Table 2

Sample			Respective detergent concentration in running buffer (mM)	Micelle molar mass (kDa)	Superdex 200 dimensions
Detergent	Concentration (mM)	Volume (µl)			
DPC	8	5	3	20.2 ± 3.2	5/150
DPC	55	100	50	16.8 ± 1.8	10/300
SDS	16	30	10	17.2 ± 3.4	2x 5/150
SDS	80	30	30	6.9 ± 3.1	2x 5/150